

Selectivity Enhancement in Dynamic Kinetic Resolution of Secondary Alcohols through Adjusting the Micro-Environment of Metal Complex Confined in Nanochannels: A Promising Strategy for Tandem Reactions

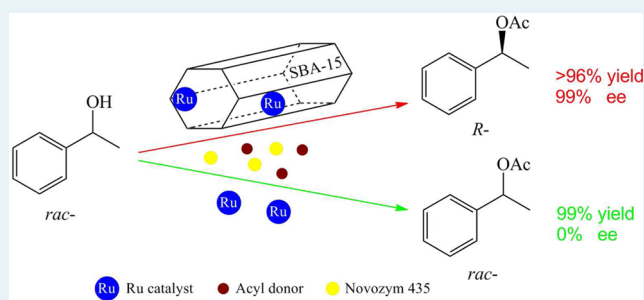
Hui Cao, Xiao-Han Zhu, Dong Wang, Zhenkun Sun, Yonghui Deng, Xiu-Feng Hou,* and Dongyuan Zhao

Department of Chemistry, Fudan University, Shanghai 200433, China

S Supporting Information

ABSTRACT: Dichloro(η^6 -*p*-cymene) (1-butyl-3-cyclohexylimidazolin-2-ylidene) ruthenium(II) (**RuL**) was synthesized and confirmed. Five heterogeneous catalysts with similar ruthenium cores were prepared by chemical immobilization method using various silica-based supports, including mesoporous silica SBA-15 of different pore sizes (**Ru/Si-9**, **Ru/Si-8**, and **Ru/Si-7**), nonporous silica particles (**Ru/SiO₂**), and surface trimethylsilylated SBA-15 (**Ru/SiMe**). The dynamic kinetic resolution (DKR) of 1-phenylethanol, which includes metal–enzyme bicatalytic racemization in tandem with stereoselective acylation, gave product in 99% yield and 0% ee with homogeneous catalyst **RuL**, whereas the heterogeneous **Ru/Si-8** exhibited high catalytic activity and enantioselectivity (up to 96% yield and 99% ee). The racemization and acylation abilities of different catalysts were analyzed. The influences of pore size and surface properties for heterogeneous catalysts were investigated, and the nanocage effect was found to be the key factor in stereoselectivity. The catalyst **Ru/Si-8** performed well in reactions with various substrates and can be reused for at least seven times.

KEYWORDS: stereoselectivity, homogeneous, heterogeneous, immobilization, ruthenium, *N*-heterocyclic carbene, tandem reaction



1. INTRODUCTION

The control of selectivity is very important for organic synthesis, especially for those catalyzed by transition metal complexes, as they can often catalyze more than one chemical reaction from the same starting materials.¹ To enhance the selectivity of metal catalysts, the most common way is to tune the steric and electronic properties of metal complexes through ligand modification.² Such a process is usually time-consuming and laborious. On the other hand, in living systems, active catalysts are confined in different regions of the cell in order to selectively synthesize various organic molecules.³ The semi-permeable cell membrane is crucial in these systems, which can not only decrease unwanted interaction between catalysts but also prevent catalysts to contact undesirable reactants. Could we mimic Nature's strategy to achieve selectivity by controlling the reaction environment instead of modification of the catalyst itself? Tremendous effort has been dedicated to the immobilization of homogeneous complexes onto a solid support over last two decades.⁴ These catalysts can be recycled and easily removed from the reaction mixture, and even provide an enhancement of the reactivity. However, there are very few examples which involve the control of selectivity in tandem reactions through adjusting space size and surface properties.⁵

Ruthenium(II) *N*-heterocyclic carbene (NHC) complexes bearing pentamethylcyclopentadienyl ligands (Cp^*) have been proven to be highly efficient in racemization of chiral alcohols.⁶ However, successful DKR with Ru carbene complexes, to the best of our knowledge, have not been reported yet. During our investigation of the catalytic performance of a cymene ruthenium NHC complex,⁷ we found that it was highly active for racemization of optically pure alcohols. However, when it was applied in DKR reaction,⁸ no enantioselectivity was observed. Surprisingly, when we used *N*-heterocyclic carbene ruthenium complex supported by mesoporous material, high enantioselectivity was achieved. Herein, we demonstrate a novel example in which the selectivity of tandem reaction is dramatically enhanced via changing the reaction environment of the catalyst centers. Furthermore, the correlation between the properties of the support and the enantioselectivity of the products is also investigated.

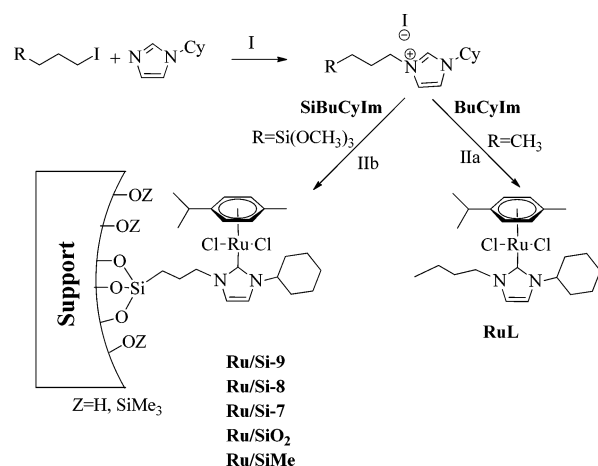
Received: July 12, 2014

Revised: November 4, 2014

Published: November 7, 2014

2. RESULTS AND DISCUSSION

2.1. Preparation of Ruthenium Complex and Silica-Supported Ruthenium Species. As shown in Scheme 1,

Scheme 1. Synthesis of Ruthenium Complex and Silica-Immobilized Species^a

^a(I) toluene, reflux, 24 h; (IIa) Ag₂O, CH₂Cl₂, 3 h; then [Ru(*p*-cymene)Cl₂]₂, 4 h; (IIb) Ag₂O, 4 Å MS, CH₂Cl₂, 12 h; then [Ru(*p*-cymene)Cl₂]₂, 16 h; then silica material, toluene, reflux, 48 h.

ruthenium complex, dichloro(η^6 -*p*-cymene) (1-butyl-3-cyclohexyl-imidazolin-2-ylidene)ruthenium(II) (**RuL**), was synthesized from the imidazolium salt 1-butyl-3-cyclohexyl-imidazolium iodide (**BuCyIm**) according to the Ag₂O method^{17c,9} using [Ru(*p*-cymene)Cl₂]₂ as a metalation reagent. The formation of **RuL** was confirmed by NMR spectroscopy. Silica-supported ruthenium species were prepared from the imidazolium salt 3-cyclohexyl-1-[3-(trimethoxysilyl)propyl]-imidazolium iodide (**SiBuCyIm**) using a similar method, followed by the addition of different supports. As mesoporous silica materials possess large surface area with high porosity and adjustable pore size, they are excellent supports for immobilization of catalysts.¹⁰ In this study, 2D hexagonally ordered mesoporous silica SBA-15 materials with hydrophilic surface and different pore sizes of 9, 8, and 7 nm, respectively, were synthesized and employed as supports for immobilization of ruthenium species, and the obtained heterogeneous catalysts were denoted as **Ru/Si-9**, **Ru/Si-8**, and **Ru/Si-7**, respectively. For comparison, catalysts supported with nonporous silica particles with a mean diameter of 20 nm and trimethylsilylated SBA-15¹¹ with hydrophobic surface and pore size of ~8 nm were also synthesized (denoted as **Ru/SiO₂** and **Ru/SiMe**, respectively). In all cases, immobilization renders the ruthenium catalysts higher tolerance against air and moisture.

2.2. Structural Characterization of Silica-Supported Ruthenium Species. Because the preparation strategy of these silica-supported ruthenium species relied on tethering ruthenium NHC to the supports via siloxy group linked with the NHC ligands, the ruthenium NHC moiety, silica framework, and pore of the supports would be retained^{7c} and were characterized by various physicochemistry methods. In the FT-IR spectra of the catalysts, the characteristic bands of silica materials around 1090 and 460 cm⁻¹ for $\nu(\text{Si-O})$ and $\delta(\text{Si-O})$ were observed, and some new bands appeared at ~2970 and ~2860 cm⁻¹, probably assigned to ruthenium NHC moiety^{7c,11} (Figure 1).

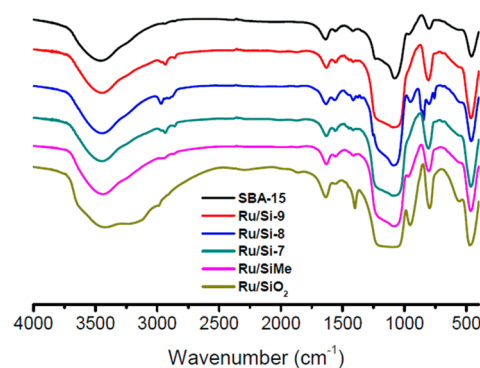


Figure 1. FT-IR spectra of **Ru/Si-9**, **Ru/Si-8**, **Ru/Si-7**, **Ru/SiMe**, **Ru/SiO₂** and SBA-15.

The solid-state ¹³C CP/MAS NMR spectra provided further evidence for the presence of ruthenium NHC moiety on the support. Strong signals at 13–35 ppm were attributed to the saturated carbons of cyclohexyl, the linker, and the cymene, whereas resonances at ~130 ppm were assigned to the unsaturated carbons of ruthenium NHC moiety, which were consistent with those of complex **RuL**. In the case of **Ru/SiMe**, signals at around 0.8 ppm were assigned to trimethylsilylated carbon^{4i,11b} (Figure 2).

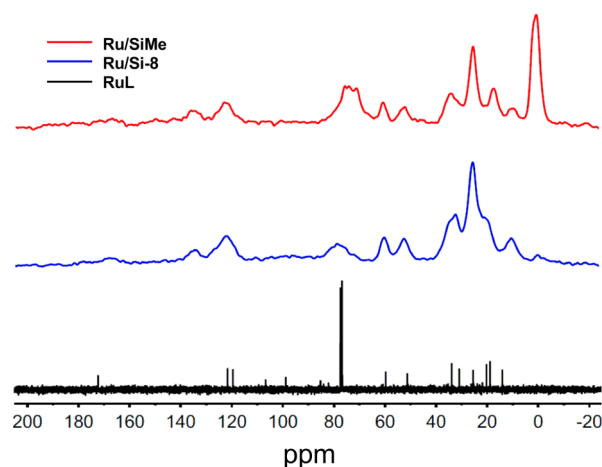


Figure 2. Solid-state ¹³C CP/MAS NMR spectra of **Ru/SiMe**, **Ru/Si-8** and ¹³C NMR spectrum of **RuL** in CDCl₃.

Solid-state ²⁹Si CP/MAS NMR spectra showed strong signals (~ -110 ppm) originating from network structures of SBA-15 and weak signals (~ -57 ppm) derived from silylether groups of ruthenium complex moiety, confirming that ruthenium NHC moieties are tethered to the supports.^{4i,11b,12} For **Ru/SiMe**, signals at around 12 ppm were assigned to methylated silicon¹³ (Figure 3).

In the small-angle X-ray scattering (SAXS) patterns of these ruthenium modified silica, **Ru/Si-9**, **Ru/Si-8**, **Ru/Si-7** and **Ru/SiMe** all displayed the characteristic peaks of SBA-15, and no peaks were observed in **Ru/SiO₂** (Figure 4).

The TEM characterization further confirmed that **Ru/Si-9**, **Ru/Si-8**, **Ru/Si-7**, and **Ru/SiMe** possess well-ordered mesostructure with two-dimensional-hexagonal arrangement of mesopores and **Ru/SiO₂** had a spherical morphology (Figure 5). Elemental mapping and EDX analysis of **Ru/Si-8** revealed a

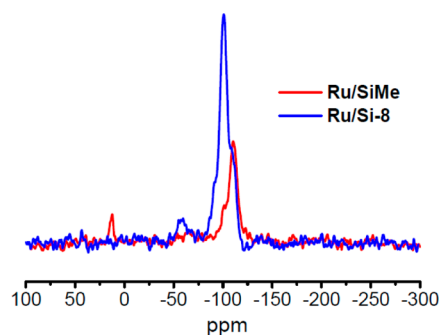


Figure 3. Solid-state ^{29}Si CP/MAS NMR spectra of Ru/Si-8 and Ru/SiMe.

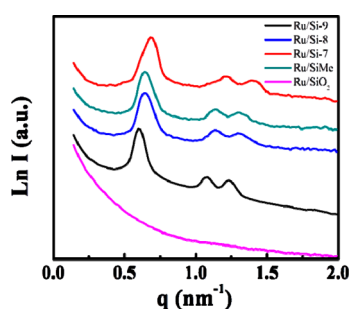


Figure 4. SAXS patterns of Ru/Si-9, Ru/Si-8, Ru/Si-7, Ru/SiMe, and Ru/SiO₂.

homogeneous distribution of Ru atoms in the silica framework (Figure 6).

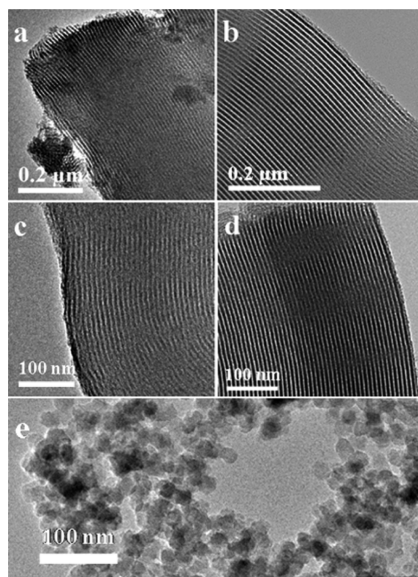


Figure 5. TEM images of (a) Ru/Si-9, (b) Ru/Si-8, (c) Ru/Si-7, (d) Ru/SiMe viewed along [001] directions and (e) silica nanoparticles Ru/SiO₂.

For further understanding of pore structures of silica-supported catalysts, the nitrogen sorption–desorption isotherms of the corresponding samples were investigated along with the BJH pore size distributions (Figure S17). The typical type IV isotherms with a characteristically adsorption–desorption hysteresis loop of the SBA-15¹⁴ were maintained for Ru/Si-9, Ru/Si-8, Ru/Si-7, and Ru/SiMe after chemical

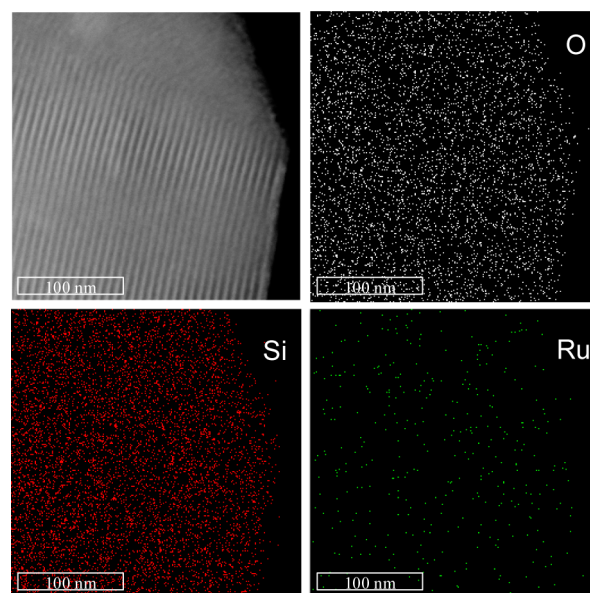


Figure 6. Elemental analysis maps for Ru/Si-8.

immobilization. Their mean pore diameters were 8.8, 7.4, 6.5, and 8.2 nm, respectively. The results of Ru/SiO₂ showed nonporous structure.

The loading amounts of grafted ruthenium are 1.2, 1.5, 2.0, 0.76, and 0.40 wt % for Ru/Si-9, Ru/Si-8, Ru/Si-7, Ru/SiMe, and Ru/SiO₂, respectively, as determined by inductively coupled plasma optical emission spectrometer (ICP). The pore diameters, pore volumes, BET specific surface areas of the supported ruthenium catalysts are summarized in Table 1.

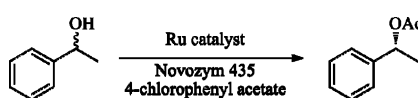
Table 1. Physicochemical properties of silica-supported Ru catalysts

catalyst	d_{pore}^a (nm)	V_{pore} (cm ³ g ⁻¹)	S_{BET} (m ² g ⁻¹)
Ru/Si-9	8.8	0.88	721
Ru/Si-8	7.4	0.64	319
Ru/Si-7	6.5	0.51	487
Ru/SiMe	8.2	0.65	322
Ru/SiO ₂	-	0.05	6.3

^aCalculated from the desorption branch of the isotherm using the BJH model.

We chose the DKR of 1-phenylethanol as a model tandem reaction, applying ruthenium complex and silica-supported ruthenium species as metal catalysts, the immobilized *Candida antarctica* lipase B (Novozym 435) as an enzymatic catalyst, 4-chlorophenyl acetate as acyl donor. The results are compiled in Table 2.

When ruthenium complex RuL was used as the metal catalyst, 1-phenylethyl acetate could be obtained with 99% isolated yield within 48 h at 60 °C, but no optical activity was observed (entry 1). On the contrary, SBA-15-supported Ru species (Ru/Si-9, Ru/Si-8, and Ru/Si-7) exhibited excellent enantioselectivity (entries 2–4). Specially, Ru/Si-8 with a pore size of ~8 nm afforded the product in 96% yield and 99% ee (entry 3). However, trimethylsilylated SBA-15-supported ruthenium catalyst Ru/SiMe with similar pore size showed lower enantioselectivity (72% ee) under the same conditions (entry 5). The nonporous silica-supported ruthenium species Ru/SiO₂ provided poor selectivity for the DKR reaction (24%

Table 2. Comparison of Ru Species Co-Catalyzed DKR of 1-Phenylethanol^a


entry	catalyst	yield [%]	ee [%]
1	RuL	99	0
2	Ru/Si-9	62	95
3	Ru/Si-8	96	99
4	Ru/Si-7	90	99
5	Ru/SiMe	70	72
6	Ru/SiO ₂	68	24

^a1-Phenylethanol (0.5 mmol), catalyst (Ru: 4 mol %), *t*-BuOK (8 mol %), Novozym 435 (20 mg), Na₂CO₃ (0.5 mmol), 4-chlorophenyl acetate (2 mmol), toluene (2.0 mL), 60 °C, 48 h. Yield was determined by ¹H NMR spectroscopy, and ee was determined by chiral HPLC.

ee, entry 6). These results indicate that immobilization of ruthenium NHC complex onto mesoporous silica with certain environment and pore size can remarkably enhance the stereoselectivity of ruthenium catalyst in the bicatalytic tandem reaction.

2.3. Microreactor Function of the Mesoporous Silica-Supported Ruthenium Catalysts. In the metal–enzyme bicatalytic DKR process, it is crucial that the metal-catalyzed racemization is compatible with the enzyme-catalyzed stereoselective acylation (namely, resolution reaction). However, many metal complexes not only are efficient racemization catalysts but also can catalyze acylation reactions, resulting in lower optical purities of the acetate products.^{8e} In order to rationalize the function of support in silica-supported ruthenium catalysts, we examined the catalytic performance of these silica immobilized ruthenium species and homogeneous ruthenium complex in racemization of (*R*)-1-phenylethanol and acylation of 1-phenylethanol.

As shown in Table 3, complex RuL was a highly efficient racemization catalyst, and (*R*)-1-phenylethanol was fully

Table 3. Ru-Catalyzed Racemization of (*R*)-1-Phenylethanol and Acylation of 1-Phenylethanol

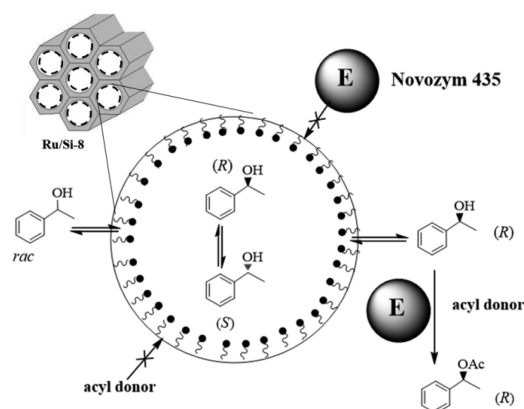
entry	catalyst	racemization ^a ee [%]	acylation ^b yield [%]
1	RuL	0	99
2	Ru/Si-9	74	0
3	Ru/Si-8	37	0
4	Ru/Si-7	28	0
5	Ru/SiMe	83	85
6	Ru/SiO ₂	71	90
7	SBA-15	97	0
8	-	98	0

^a(*R*)-1-phenylethanol (97% ee, 0.50 mmol), catalyst (4 mol % Ru), *t*-BuOK (8 mol %), toluene (2 mL), 60 °C, 48 h. The ee value was determined by chiral GC. ^b1-Phenylethanol (0.5 mmol), catalyst (Ru: 4 mol %), *t*-BuOK (5 mol %), Na₂CO₃ (0.5 mmol), isopropenyl acetate (2 mmol), toluene (2.0 mL), 25 °C, 4 h. Isolated yields.

racemized within 48 h. However, it was also highly efficient for acylation of 1-phenylethanol (entry 1), a competitive reaction, which could be the key reason for the decrease of enantioselectivity of the DKR product. On the other hand, for all SBA-15-supported ruthenium species, Ru/Si-9, Ru/Si-8,

and Ru/Si-7, the racemization efficiency decreased with increasing pore size,¹⁵ whereas the Ru-catalyzed acylation was totally suppressed (entries 2–4). Catalysts supported on SBA-15 exhibited selectivity over racemization and acylation. As ruthenium active center is located in the channel of mesoporous silica, all Ru-catalyzed reactions have to proceed in the mesoporous nanocage of SBA-15. The fact that no acylation reaction was observed with the SBA-15-supported Ru/Si-9, Ru/Si-8, and Ru/Si-7 suggested that the acyl donor can hardly entered the nanocage, thus leading to exclusive selectivity for racemization reaction. When we applied the nonporous Ru/SiO₂ as catalyst, substantial acylation product was observed (entry 6). These indicated the crucial role of supporting mesoporous material in selectivity.

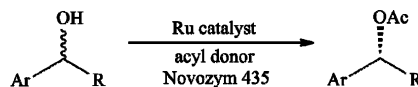
Considering the effect of the pore size on Ru-catalyzed acylation is minimal, we speculated that the hydrophilicity of mesoporous silica support SBA-15 might be the cause for the selectivity over acylation reaction. The hydrophilic surface of SBA-15 is advantageous to let alcohols into the nanocage. On the contrary, hydrophobic acyl donors are kept outside of the nanocage and undergo stereoselectively enzyme-catalyzed acylation, affording optical pure acetate product (Scheme 2).

Scheme 2. Selectivity of SBA-15-Supported Ru Species Co-Catalyzed DKR Reaction

In order to verify our speculation, methylsilylated SBA-15-supported ruthenium catalyst Ru/SiMe with similar pore size to Ru/Si-8 but hydrophobic pore channels was applied. As we speculated, Ru/SiMe turned to be an efficient acylation catalyst with poor racemization performance (entry 5), suggesting that the hydrophilicity of the nanocage is responsible for enhanced selectivity in the DKR process. Control experiments indicated that SBA-15 or the base alone does not cause racemization or acylation (entries 7–8).

2.4. Substrate Scope in the Presence of Ru/Si-8. To demonstrate the generality of this strategy, the hydrophilic nanocatalyst Ru/Si-8 was applied in DKR of various secondary alcohols and then compared with the RuL system (Table 4).

The Ru/Si-8-co-catalyzed DKR reactions afforded products in 89–99% yield and 90–99% ee (entries 1–5), which is completely different from the corresponding RuL system with 0% ee value for these *sec*-alcohols (entries 1–5). Substituent effect on the reaction of benzylic alcohols was not significant. Similar to 1-phenylethanol, 1-(naphthalen-2-yl)ethanol (entry 6), 1-phenylpropan-1-ol (entry 7), and 1,2,3,4-tetrahydronaphthalen-1-ol (entry 8) all gave excellent yields and ee values. Especially, the aliphatic alcohol (entry 9), which formed after

Table 4. Ru/Si-8 or RuL in DKR of Various *sec*-Alcohols^a


entry	product (Ar, R)	Ru-catalyst	time (h)	yield ^b (%)	ee ^c (%)
1	Ph, Me	Ru/Si-8	48	96	>99
		RuL	0.5	96	0
2	<i>p</i> -MeOPh, Me	Ru/Si-8	48	91	98
		RuL	4	89	0
3	<i>p</i> -MePh, Me	Ru/Si-8	48	89	99
		RuL	4	99	0
4	<i>p</i> -ClPh, Me	Ru/Si-8	48	99	99
		RuL	4	99	0
5	<i>p</i> -BrPh, Me	Ru/Si-8	48	99	97
		RuL	4	99	0
6	2-naphthyl, Me	Ru/Si-8	48	95	99
		RuL	4	93	0
7	Ph, Et	Ru/Si-8	48	90	99
		RuL	4	90	0
8	1,2,3,4-tetra-hydronaphthyl	Ru/Si-8	72	89	99
		RuL	10	91	0
9	2-phenylethyl, Me	Ru/Si-8	72	93	97
		RuL	8	93	0

^aAlcohols (1.0 mmol), acyl donor (3.0 equiv), *t*-BuOK (8 mol %), Ru-catalyst (4 mol %), Novozym 435 (20 mg), Na₂CO₃ (1.0 equiv), toluene (3.0 mL), 60 °C. For Ru/Si-8: 4-chlorophenyl acetate; RuL: isopropenyl acetate. ^bDetermined by ¹H NMR spectroscopy for Ru/Si-8. Isolated yield for RuL. ^cDetermined by chiral HPLC on pure acetates.

hydrolysis of the esters, was not readily accessible by asymmetric reduction of the corresponding ketone, also gave excellent yield and enantioselectivity after a longer reaction time.

2.5. Catalyst Recovery and Reuse. Because both Ru/Si-8 and Novozym 435 were solid catalysts, they could be readily separated from the reaction mixture through simple filtration and reused for the DKR process. The reusability of Ru/Si-8 was tested in the DKR of 1-phenylethanol under conditions similar to those for entry 1 of Table 4: first run, 96%, > 99% ee; second run, 95%, > 99% ee; third run, 64%, > 99% ee. Considering the decreased enzyme activity¹⁶ might be the cause of the yield drop, a small amount of fresh Novozym 435 was added before each cycle. In this case, the recovered catalyst could be reused at least seven times with NMR yields of 96, 95, 96, 94, 92, 90, and 74% and ee values >99% for all the seven consecutive runs. After six runs, the reaction mixture already became a thick suspension, and the yield drop in the seventh run is likely due to inefficient stirring. ICP measurements indicated that less than 4% of the ruthenium atom leached from the catalyst Ru/Si-8 during each catalytic cycle.

3. CONCLUSIONS

We successfully designed and prepared a series of Ru-supported mesoporous silica materials, which have hydrophilic or hydrophobic environments and different pore sizes. With metal–enzyme bicatalytic DKR of alcohols as the probe reaction, we demonstrated that the selectivity for the tandem reaction was remarkably enhanced through confining metal catalyst core in the nanocage. Comparing ordered mesoporous supports and nonporous silica, we have shown that the

mesoporous silica-supported ruthenium catalyst could behave as a microreactor with selective catalysis function. The selectivity of metal-complex-catalyzed tandem DKR reaction could be controlled by tuning the surface property and pore size of the nano support. Our strategy offers an alternative and attractive method for the enhancement of selectivities in tandem reactions through adjusting the microenvironment of metal catalysts.

4. EXPERIMENTAL SECTION

General. All manipulations were carried out under a nitrogen atmosphere using standard Schlenk techniques unless otherwise stated. Solvents were distilled under nitrogen from sodium benzophenone (hexane, diethyl ether, toluene) or calcium hydride (dichloromethane), and methanol was distilled over Mg/I₂. The starting materials 1-cyclohexylimidazole,¹⁷ [Ru(*p*-cymene)Cl₂]₂,¹⁸ mesoporous silica SBA-15,¹⁰ silica nanoparticles¹⁰ and surface-methylsilylated SBA-15¹¹ were synthesized according to the literature procedures. Other chemical reagents were obtained from commercial sources and used without further purification.

Characterization. Ru loading amounts in the catalysts were analyzed using an inductively coupled plasma optical emission spectrometer (ICP, Varian VISTA-MPX). FT-IR spectra were recorded on a Nicolet AVATAR-360 IR spectrometer using KBr disc in the range of 4000–400 cm⁻¹. NMR spectra were recorded using Bruker spectrometers operating at 400 (¹H) MHz and 100 MHz (¹³C) in CDCl₃. Solid-state ¹³C and ²⁹Si CP MAS NMR spectra were recorded at 100.6 MHz using a Bruker AV-400 spectrometer. Morphology and elemental mapping of the materials were observed on a JEOL JEM 2100F transmission electron microscope (TEM) with energy-dispersive X-ray (EDX) spectroscopy using an accelerating voltage of 200 kV. The scattering (SAXS) measurements were taken on a Nanostar Small angle X-ray scattering system (Bruker, Germany) using Cu K α radiation (40 kV, 35 mA). Nitrogen adsorption isotherms were measured at 77 K after being outgassed at 383 K overnight on a Quantachrome Nova 4000 analyzer. Pore size distributions and specific surface areas (*S*_{BET}) were calculated using the BJH model and the BET method, respectively. Enantiomeric excesses were determined by chiral HPLC equipped with a capillary column Daicel OD-H or chiral GC equipped with a capillary column Varian CP 7502.

Preparation of Homogeneous Catalyst RuL. 1-Cyclohexylimidazole (150 mg, 1.0 mmol) was refluxed with 1-iodobutane (150 μ L, 2.2 mmol) in toluene for 24 h, during which time the product precipitated. After the product was cooled to room temperature, it was filtered, and the precipitate was washed with diethyl ether and dried under vacuum to afford the corresponding imidazolium iodide BuCyImI: White solid, yield: 95%. ¹H NMR (CDCl₃, 400 MHz): δ 9.92 (s, 1H, N-CH-N), 7.49 (d, *J* = 12 Hz, 2H, NCHCHN), 4.35 (m, 1H, N-CH), 4.27 (t, 2H, N-CH₂), 2.10 (m, 2H, CH₂ of *n*-Bu), 1.78–1.15 (m, 12H), 0.81 (t, 3H, CH₃ of *n*-Bu); ¹³C NMR (CDCl₃, 100 MHz): δ 134.90 (NCHN), 122.43 (NCHCHN), 120.77 (NCHCHN), 59.97 (NCH), 49.82 (NCH₂), 33.51 (Cy), 32.26 (CH₂), 24.86, 24.49, 19.44, 13.53. To a solution of BuCyImI (50 mg, 0.15 mmol) in 15 mL of dry CH₂Cl₂, Ag₂O (20 mg, 0.08 mmol) was added in the absence of light and stirred under nitrogen for 3 h. After the addition of [Ru(*p*-cymene)Cl₂]₂ (45 mg, 0.074 mmol), the mixture was stirred for another 4 h at room temperature in the dark. The precipitate was filtered off, and the filtrate was concentrated under vacuum.

The product (**RuL**) was obtained by adding of petroleum ether to CH_2Cl_2 solution. **RuL**: Yellow solid, yield: 64%. ^1H NMR (CDCl_3 , 400 MHz): δ 7.04 (s, 2H, NCHCHN), 5.39 (d, J = 22.2 Hz, 2H, $\text{Ph}_{\text{cymene}}$), 5.08 (d, J = 29.2 Hz, 2H, $\text{Ph}_{\text{cymene}}$), 4.84 (m, 1H, CH_{Cy}), 4.62 (br, 1H, CH_2N), 3.90 (br, 1H, CH_2N), 2.91–2.83 (m, 1H, $\text{CH}_{\text{cymene}}$), 2.06 (s, 3H, $\text{CH}_{3\text{cymene}}$), 2.05–1.08 (m, 14H, $\text{CH}_{2\text{Bu,Cy}}$), 1.27, 1.26 (s, 6H, $\text{CH}_{3\text{cymene}}$), 0.95 (m, 3H, $\text{CH}_{3\text{Bu}}$). ^{13}C NMR (CDCl_3): δ 172.32, 121.63, 119.51, 106.75, 98.86, 85.31, 85.23, 82.13, 82.11, 59.72, 51.31, 33.89, 30.96, 26.26, 26.23, 25.53, 25.40, 25.37, 23.87, 21.87, 20.89, 18.83, 14.08.

Preparations of Heterogeneous Catalysts. To a 50 mL Schlenk tube containing 10 mL of toluene was added 1-cyclohexylimidazole (75 mg, 0.50 mmol) and 3-iodopropyltrimethoxysilane (165 mg, 0.54 mmol). The mixture was refluxed for 24 h before filtration. The precipitates were washed with diethyl ether and dried under vacuum. **SiBuCyImI**: White solid 202 mg, yield: 92%. ^1H NMR (CDCl_3 , 400 MHz): δ 10.0 (s, 1H, NCHN), 7.68 (d, 2H, $\text{NCH}_2\text{CH}_2\text{N}$), 7.54 (s, 2H, $\text{NCH}_2\text{CH}_2\text{N}$), 4.42 (m, 1H, CH_{Cy}), 3.58 (s, 9H, OCH_3), 2.25 (m, 2H, CH_2N), 2.04–1.46 (m, 10H, Cy), 1.33 (m, 2H, CH_2), 0.67 (m, 2H, SiCH_2). ^{13}C NMR (CDCl_3): δ 135.0, 122.2, 120.8, 60.0, 51.7, 50.8, 33.5, 24.8, 24.5, 24.2, 5.9. The imidazolium salt **SiBuCyImI** (200 mg, 0.45 mmol) was dissolved in CH_2Cl_2 (10 mL) and added to a Schlenk vessel containing activated 4 Å molecular sieves (50 mg) and Ag_2O (63 mg, 0.27 mmol). The reaction mixture was stirred at room temperature for 12 h in the absence of light. Then $[\text{Ru}(\text{p-cymene})\text{Cl}_2]_2$ (220 mg, 0.36 mmol) was added, and it was stirred for another 12 h. After filtration, the filtrate was dried under vacuum and added into the suspension of 2 g of SBA-15 (8 nm) in toluene (10 mL). After the mixture was refluxed for 48 h, the resulting solid was filtered and washed with CH_2Cl_2 and ether, and then vacuum-dried to obtain **Ru/Si-8**.

Ru/Si-9, Ru/Si-7, Ru/SiO₂, and Ru/SiMe were prepared in similar method using SBA-15 (9 and 7 nm), SiO_2 nanoparticles (20 nm), and methylated SBA-15 (8 nm).

General Procedure for Racemization of (R)-1-Phenylethanol. To a 25 mL Schlenk tube, catalyst (4 mol % Ru), *t*-BuOK (8 mol %), and toluene (2 mL) were added. After 10 min of stirring, (R)-1-phenylethanol (97% ee, 0.50 mmol) was added to the reaction mixture and stirred at 60 °C for 48 h. After toluene was removed, the residue was extracted with petroleum ether. The extract was subjected to chiral GC analysis.

General Procedure for Chemical Acylation of 1-Phenylethanol. In a typical reaction, *t*-BuOK (8 mol %) and catalyst (4 mol % Ru) was added to a 25 mL Schlenk tube containing 2 mL toluene and stirred for 10 min. Sodium carbonate (0.5 mmol), 1-phenylethanol (0.5 mmol), isopropenyl acetate (2 mmol) were then added, and the mixture was stirred at room temperature for 4 h. The reaction mixture was concentrated, and the residue was purified by column chromatography with petroleum ether.

General Procedure for DKR of sec-Alcohols. In a typical reaction, *t*-BuOK (8 mol %) and catalyst (4 mol % Ru) was added to a 25 mL Schlenk tube containing 2 mL toluene and stirred for 10 min. Sodium carbonate (0.5 mmol), *sec*-alcohol (0.5 mmol), acylating agent (2–3 mmol), and Novozym-435 (20 mg) were then added. After being stirred at 60 °C for 48 h, the reaction mixture was filtered and evaporated, then extracted with petroleum ether. The extract was subjected to ^1H NMR¹⁹ and chiral HPLC analysis.

General Procedure for Ru/Si-8 Recycling Use. According to the general procedure for DKR of 1-phenylethanol, the first run reaction was carried out. After completion of the reaction, the solids were filtrated, washed by CH_2Cl_2 and water, and then vacuum-dried. The recovered catalyst was used for consecutive reactions under same condition, and 6 mg of Novozym-435 was added each time.

■ ASSOCIATED CONTENT

Supporting Information

The following file is available free of charge on the ACS Publications website at DOI: 10.1021/cs500988a.

NMR spectra, solid-state ^{13}C -, ^{29}Si - NMR spectra, N_2 sorption–desorption isotherms, chromatograms, and NMR data of products (PDF)

■ AUTHOR INFORMATION

Corresponding Author

*E-mail: xfhou@fudan.edu.cn.

Notes

The authors declare no competing financial interest.

■ ACKNOWLEDGMENTS

Financial support by the National Science Foundation of China (grant nos. 20871032, 20971026, and 21271047) and by the Shanghai Leading Academic Discipline Project (project no. B108) is gratefully acknowledged.

■ REFERENCES

- (1) (a) Fogg, D. E.; dos Santos, E. N. *Coord. Chem. Rev.* **2004**, *248*, 2365–2379. (b) Farina, V.; Reeves, J. T.; Senanayake, C. H.; Song, J. J. *Chem. Rev.* **2006**, *106*, 2734–2793. (c) Parashar, R. K. *Synthetic Strategies. In Reaction Mechanisms in Organic Synthesis*; John Wiley & Sons, Inc.: West Sussex, United Kingdom, 2008; Chapter 1.
- (2) (a) Albrecht, L.; Jiang, H.; Jørgensen, K. A. *Angew. Chem., Int. Ed.* **2011**, *50*, 8492–8509. (b) Climent, M. J.; Corra, A.; Iborra, S. *Chem. Rev.* **2011**, *111*, 1072–1133.
- (3) (a) Ovádi, J.; Sreter, P. A. *Int. Rev. Cytol.* **1999**, *192*, 255–280. (b) Nakano, S.; Miyoshi, D.; Sugimoto, N. *Chem. Rev.* **2014**, *114*, 2733–2758.
- (4) For reviews on immobilized complexes, see: (a) Fraile, J. M.; García, J. I.; Herreras, C. I.; Mayoral, J. A. *Chem. Soc. Rev.* **2009**, *38*, 695–706. (b) Thomas, J. M.; Raja, R. *Acc. Chem. Res.* **2008**, *41*, 708–720. (c) Zaera, F. *Chem. Soc. Rev.* **2013**, *42*, 2746–2762. For recent progresses in immobilized complexes, see: (d) Copéreta, C. J.; Basseta, M. *Adv. Synth. Catal.* **2007**, *349*, 78–92. (e) Drozdak, R.; Allaert, B.; Ledoux, N.; Dragutan, I.; Dragutan, V.; Verpoort, F. *Adv. Synth. Catal.* **2005**, *347*, 1721–1743. (f) Tada, M.; Muratsugu, S.; Kinoshita, M.; Sasaki, T.; Iwasawa, Y. *J. Am. Chem. Soc.* **2010**, *132*, 713–724. (g) Li, B.; Bai, S.; Wang, X.; Zhong, M.; Yang, Q.; Li, C. *Angew. Chem., Int. Ed.* **2012**, *51*, 11517–11521. (h) Jones, M. D.; Raja, R.; Thomas, J. M.; Johnson, B. F. G.; Lewis, D. W.; Rouzaud, J.; Harris, K. D. M. *Angew. Chem., Int. Ed.* **2003**, *42*, 4326–4331. (i) Liu, G.; Wang, J.; Huang, T.; Liang, X.; Zhang, Y.; Li, H. *J. Mater. Chem.* **2010**, *20*, 1970–1975. (j) Liu, P. N.; Deng, J. G.; Tu, Y. Q.; Wang, S. H. *Chem. Commun.* **2004**, 2070–2071. (k) Yang, Q.; Ma, S.; Li, J.; Xiao, F.; Xiong, H. *Chem. Commun.* **2006**, 2495–2497. (l) Yang, Y.; Rioux, R. M. *Chem. Commun.* **2011**, 6557–6559. (m) Zhi, J.; Song, D.; Li, Z.; Lei, X.; Hu, A. *Chem. Commun.* **2011**, 10707–10709. (n) Liu, P.; Zhou, C.-Y.; Xiang, S.; Che, C.-M. *Chem. Commun.* **2010**, 2739–2741.
- (5) (a) Liu, R.; Jin, R.; An, J.; Zhao, Q.; Cheng, T.; Liu, G. *Chem.—Asian J.* **2014**, *9*, 1388–1394. (b) Wang, Y.; Su, N.; Ye, L.; Ren, Y.; Chen, X.; Du, Y.; Li, Z.; Yue, B.; Tsang, S. E.; Chen, Q.; He, H. *J. Catal.* **2014**, *313*, 113–126.

(6) (a) Bosson, J.; Nolan, S. P. *J. Org. Chem.* **2010**, *75*, 2039–2043. (b) Nun, P.; Fortman, G. C.; Slawin, A. M. Z.; Nolan, S. P. *Organometallics* **2011**, *30*, 6347–6350. (c) Balogh, J.; Slawin, A. M. Z.; Nolan, S. P. *Organometallics* **2012**, *31*, 3259–3263.

(7) (a) Zhong, R.; Wang, Y.-N.; Guo, X.-Q.; Chen, Z.-X.; Hou, X.-F. *Chem.—Eur. J.* **2011**, *17*, 11041–11051. (b) Hou, X.-F.; Wang, Y.-N.; Göttker-Schnetmann, I. *Organometallics* **2011**, *30*, 6053–6056. (c) Guo, X.-Q.; Wang, Y.-N.; Wang, D.; Cai, L.-H.; Chen, Z.-X.; Hou, X.-F. *Dalton Trans.* **2012**, *41*, 14557–14567. (d) Wang, D.; Guo, X.-Q.; Wang, C.-X.; Wang, Y.-N.; Zhong, R.; Zhu, X.-H.; Cai, L.-H.; Gao, Z.-W.; Hou, X.-F. *Adv. Synth. Catal.* **2013**, *355*, 1117–1125. (e) Zhu, X.-H.; Cai, L.-H.; Wang, C.-X.; Wang, Y.-N.; Guo, X.-Q.; Hou, X.-F. *J. Mol. Catal. A: Chem.* **2014**, *393*, 134–141.

(8) (a) Pàmies, O.; Bäckvall, J.-E. *Chem. Rev.* **2003**, *103*, 3247–3261. (b) Ahn, Y.; Ko, S.-B.; Kim, M.-J.; Park, J. *Coord. Chem. Rev.* **2008**, *252*, 647–658. (c) Pellissier, H. *Tetrahedron* **2011**, *67*, 3769–3802. (d) Warner, M. C.; Bäckvall, J.-E. *Acc. Chem. Res.* **2013**, *46*, 2545–2555. (e) Hoyos, P.; Pace, V.; Alcántara, A. R. *Adv. Synth. Catal.* **2012**, *354*, 2585–2611. (f) Lee, J. H.; Han, K.; Kim, M.-J.; Park, J. *Eur. J. Org. Chem.* **2010**, 999–1015. (g) Martín-Matute, B.; Bäckvall, J.-E. *Curr. Opin. Chem. Biol.* **2007**, *11*, 226–232. (h) Choi, Y. K.; Kim, Y.; Han, Y.; Park, J.; Kim, M.-J. *J. Org. Chem.* **2009**, *74*, 9543–9545. (i) Kim, M.-J.; Kim, W.-H.; Han, K.; Choi, Y. K.; Park, J. *Org. Lett.* **2007**, *9*, 1157–1159.

(9) (a) Özdemir, I.; Gürbüz, N.; Seçkin, T.; Çetinkaya, B. *Appl. Organomet. Chem.* **2005**, *19*, 633–638. (b) Dastgir, S.; Coleman, K. S.; Green, M. L. H. *Dalton Trans.* **2011**, *40*, 661–672. (c) Karimi, B.; Enders, D. *Org. Lett.* **2006**, *8*, 1237–1240.

(10) (a) Zhao, D.; Feng, J.; Huo, Q.; Melosh, N.; Frederickson, G. H.; Chmelka, B. F.; Stucky, G. D. *Science* **1998**, *279*, 548–552. (b) Yang, P.; Zhao, D.; Margolese, D. I.; Chmelka, B. F.; Stucky, G. D.; Galen, D. *Nature* **1998**, *396*, 152–155. (c) Karimi, B.; Khorasani, M. *ACS Catal.* **2013**, *3*, 1657–1664. (d) Wu, F.; Feng, Y.; Jones, C. W. *ACS Catal.* **2014**, *4*, 1365–1375.

(11) (a) Li, L.; Shi, J.-L. *Adv. Synth. Catal.* **2005**, *347*, 1745–1749. (b) Palkovits, R.; Arlt, D.; Stepowska, H.; Schüth, F. *Chem.—Eur. J.* **2009**, *15*, 9183–9190.

(12) (a) Maishal, T. K.; Alauzun, J.; Basset, J.-M.; Copéret, C.; Corriu, R. J. P.; Jeanneau, E.; Mehdi, A.; Reyé, C.; Veyre, L.; Thieuleux, C. *Angew. Chem., Int. Ed.* **2008**, *47*, 8654–8656. (b) Sasaki, T.; Zhong, C.; Tada, M.; Iwasawa, Y. *Chem. Commun.* **2005**, 2506–2508.

(13) (a) Stein, A.; Melde, B. J.; Schroden, R. C. *Adv. Mater.* **2000**, *19*, 1403–1419. (b) Huh, S.; Wiench, J. W.; Trewyn, B. G.; Song, S.; Pruski, M.; Lin, V. S.-Y. *Chem. Commun.* **2003**, 2364–2365.

(14) Zhang, R.; Ding, W.; Tu, B.; Zhao, D. *Chem. Mater.* **2007**, *19*, 4379–4381.

(15) Kidder, M. K.; Britt, P. F.; Zhang, Z.; Dai, S.; Hagaman, E. W.; Chaffee, A. L.; Buchanan, A. C., III *J. Am. Chem. Soc.* **2005**, *127*, 6353–6360.

(16) Kim, N.; Ko, S.-B.; Kwon, M. S.; Kim, M.-J.; Park, J. *Org. Lett.* **2005**, *7*, 4523–4526.

(17) Perry, M. C.; Cui, X.; Powell, M. T.; Hou, D.-R.; Reibenspies, J. H.; Burgess, K. *J. Am. Chem. Soc.* **2003**, *125*, 113–123.

(18) Bennett, M. A.; Huang, T. N.; Matheson, T. W.; Smith, A. K. *Inorg. Synth.* **1982**, *21*, 74–78.

(19) Persson, B. A.; Larsson, A. L. E.; Ray, M. L.; Bäckvall, J.-E. *J. Am. Chem. Soc.* **1999**, *121*, 1645–1650.